Molecular profile of MSH6-associated colorectal carcinomas shows distinct features from other Lynch syndrome-associated colorectal carcinomas

Helderman, N.C.; Lam, A.S.V.'.; Morreau, H.; Boot, A.; Wezel, T. van; Nielsen, M.

Molecular Profile of *MSH6*-Associated Colorectal Carcinomas Shows Distinct Features From Other Lynch Syndrome–Associated Colorectal Carcinomas

See editorial on page 20.

Lynch syndrome (LS) is the most common hereditary colorectal cancer (CRC) syndrome and is caused by pathogenic constitutional variants in 1 of the mismatch repair (MMR) genes, including *MLH1*, *MSH2* (*EPCAM*), *MSH6*, and *PMS2*. Although generally referred to as 1 entity, LS exhibits a highly heterogeneous phenotype, exemplified by major differences in cancer penetrance between MMR gene variant carriers.[1] These differences imply that the quality of colonoscopy, optimal surveillance intervals, treatment, preventive strategies, and other aspects of care likely differ between LS subgroups. Nevertheless, in most countries all (newly) diagnosed LS patients are subject to identical screening and treatment regimes.

The study of LS CRC molecular profiles will improve our understanding of phenotypic heterogeneity and may in turn stimulate the development of gene-specific guidelines. Because previous molecular studies focused predominantly on *MLH1*-, *MSH2*-, and *PMS2*-associated CRCs, our study aimed to define the molecular profile of *MSH6*-associated CRCs relative to other LS CRCs. The study included 106 confirmed LS CRCs, of which 44 (25 *MSH6*-, 5 *MLH1*-, 5 *MSH2*-, and 9 *PMS2*-associated CRCs) were analyzed by whole exome sequencing (WES) and 62 (24 *MLH1*-, 18 *MSH2*-, and 20 *PMS2*-associated CRCs) by a cancer hotspot panel (CHP) described previously.[2] For a full description of the materials and methods used, refer to the Supplementary Methods. A description of the total cohort, consisting of both WES and CHP cohorts, is presented in Supplementary Table 1. A full description of all available histologic and molecular characteristics (including constitutional MMR and somatic variants) for each analyzed LS CRC is presented in Supplementary Table 2.

Although the overall variant spectra of *MSH6*-, *MLH1*-, *MSH2*-, and *PMS2*-associated CRCs look similar, notable differences exist. These include the higher ($P < .01$) overall number of deficient MMR (dMMR) signature-associated single nucleotide variants (SNVs) and the lower ($P = .01$) overall number of dMMR signature-associated insertion/deletion variants (INDELs) in *MSH6*-associated CRCs vs *PMS2*-associated CRCs (Figure 1*A*–*C*, Supplementary Table 1). One possible explanation for these findings is the specific protein function during MMR: although the PMS2–MLH1 complex (hMutLα) is essential for the repair of SNVs and INDELs, the MSH2–MSH6 (hMutSα) complex is mainly involved in the repair of SNVs and is believed to be redundant for INDEL repair, which mainly depends on MSH2–MSH3 (hMutSβ).[1] Consequently, the absence of MSH6 activity likely results in the accumulation of SNVs, rather than the profound microsatellite instability (MSI; associated with INDELs) that follows MLH1, MSH2, or PMS2

dysfunction. This is further reflected by 2 microsatellite stable *MSH6*-associated CRCs with loss of MSH6 expression in our cohort and would imply that immunohistochemical MMR staining may be more sensitive than MSI testing in *MSH6*-associated CRCs.[3]

The fact that MSH6 dysfunction predominantly leads to the accumulation of SNVs, whereas PMS2 (and MLH1, MSH2) dysfunction promotes MSI is intriguing in light of the previously observed lower CRC penetrance of *PMS2* (5.9%–13%) vs *MSH6* variants (20%).[4–6] This suggests that SNVs rather than INDELs drive the development of *MSH6*-associated CRCs, thereby potentially mitigating the importance of MSI as a driving force of tumor development. Moreover, it suggests the hypothesis that *MSH6*-associated CRCs are less sensitive to immunotherapies and frameshift peptide neoantigen-based vaccines compared with other LS subgroups, because MSI is among the important biomarkers for immunotherapy response. Future studies should explore the (coding) microsatellite mutation and immune profile of *MSH6*-associated CRCs to test this hypothesis as well as stratify immunotherapy responses based on the underlying MMR gene defect.
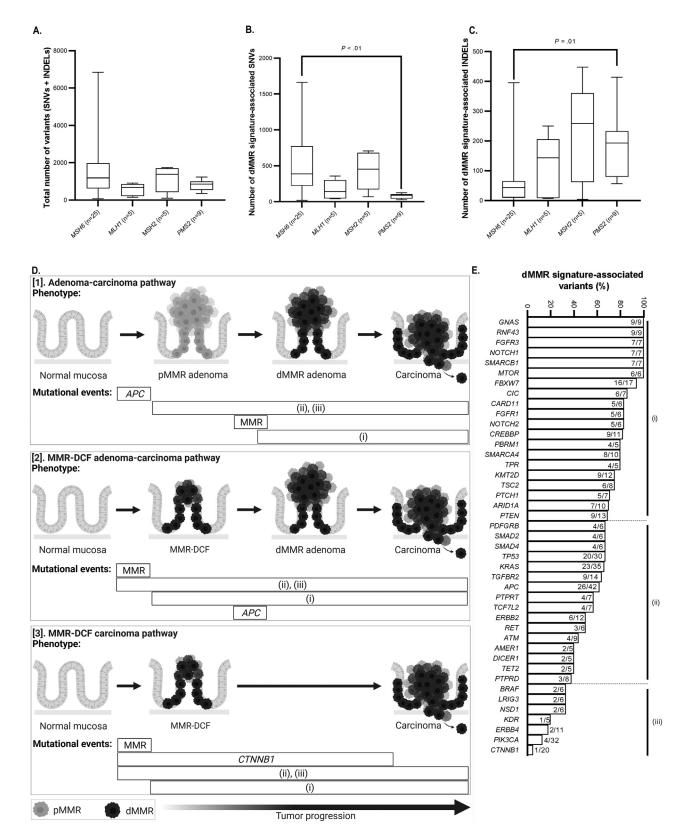
Another striking finding involved the lower abundance of *CTNNB1* variants in *MSH6*-associated CRCs (8%, 2/25) vs *MLH1*-associated CRCs (47%, 14/29; $P = .04$) (Supplementary Table 1). *CTNNB1* variants are believed to be responsible for an invasive growth pattern,[7] for instance through submucosal growth or direct tumor progression from MMR deficient crypt foci (MMR-DCF carcinoma pathway) (Figure 1*D*).[1,8,9] This invasive growth pattern may hypothetically lead to the development of postcolonoscopy CRCs, which are diagnosed after a colonoscopy in which no cancer was found. The relatively low abundance of *CTNNB1* variants in *MSH6*-associated CRCs might therefore explain the relatively low (15%) prevalence of postcolonoscopy CRCs observed among *MSH6* variant carriers[10] and illustrates that surveillance intervals may be extended for *MSH6* variant carriers. The latter has already been proposed for *PMS2* variant carriers[2] and may have resulted from the fact that current guidelines were formulated based on cohorts that primarily consisted of *MLH1* and *MSH2* variant carriers, for whom the prevalence of postcolonoscopy CRCs is remarkably higher (45%).[10]

Most current article

RESEARCH LETTERS

LS CRCs may alternatively originate from MMR-proficient adenomas (adenoma–carcinoma pathway) or from MMR-DCF through an intervening adenoma stage (MMR-DCF adenoma–carcinoma pathway).[8] These pathways have been linked to *APC* variants, which were observed in 32% of all *MSH6*-associated CRCs. Our gene-based signature analysis also cast light on the distinct pathways of LS carcinogenesis, including potential time windows for mutational events in each gene (Figure 1*E*). For instance, most *APC*, *KRAS*, and *TP53* variants in

A. Total number of variants (SNVs + INDELs) — MSH6 (n=25), MLH1 (n=5), MSH2 (n=5), PMS2 (n=9)

B. Number of dMMR signature-associated SNVs — P < .01 — MSH6 (n=25), MLH1 (n=5), MSH2 (n=5), PMS2 (n=9)

C. Number of dMMR signature-associated INDELs — P = .01 — MSH6 (n=25), MLH1 (n=5), MSH2 (n=5), PMS2 (n=9)

D.

[1]. Adenoma-carcinoma pathway
Phenotype: Normal mucosa → pMMR adenoma → dMMR adenoma → Carcinoma
Mutational events: APC; (ii), (iii); MMR; (i)

[2]. MMR-DCF adenoma-carcinoma pathway
Phenotype: Normal mucosa → MMR-DCF → dMMR adenoma → Carcinoma
Mutational events: MMR; (ii), (iii); (i); APC

[3]. MMR-DCF carcinoma pathway
Phenotype: Normal mucosa → MMR-DCF → Carcinoma
Mutational events: MMR; CTNNB1; (ii), (iii); (i)

pMMR / dMMR / Tumor progression

E. dMMR signature-associated variants (%)

Gene	Ratio	Group
GNAS	9/9	(i)
RNF43	9/9	(i)
FGFR3	7/7	(i)
NOTCH1	7/7	(i)
SMARCB1	7/7	(i)
MTOR	6/6	(i)
FBXW7	16/17	(i)
CIC	6/7	(i)
CARD11	5/6	(i)
FGFR1	5/6	(i)
NOTCH2	5/6	(i)
CREBBP	9/11	(i)
PBRM1	4/5	(i)
SMARCA4	8/10	(i)
TPR	4/5	(i)
KMT2D	9/12	(i)
TSC2	6/8	(i)
PTCH1	5/7	(i)
ARID1A	7/10	(i)
PTEN	9/13	(i)
PDFGRB	4/6	(ii)
SMAD2	4/6	(ii)
SMAD4	4/6	(ii)
TP53	20/30	(ii)
KRAS	23/35	(ii)
TGFBR2	9/14	(ii)
APC	26/42	(ii)
PTPRT	4/7	(ii)
TCF7L2	4/7	(ii)
ERBB2	6/12	(ii)
RET	3/6	(ii)
ATM	4/9	(ii)
AMER1	2/5	(ii)
DICER1	2/5	(ii)
TET2	2/5	(ii)
PTPRD	3/8	(ii)
BRAF	2/6	(iii)
LRIG3	2/6	(iii)
NSD1	2/6	(iii)
KDR	1/5	(iii)
ERBB4	2/11	(iii)
PIK3CA	4/32	(iii)
CTNNB1	1/20	(iii)

MSH6-associated CRCs were dMMR signature-associated. This suggests that these variants occurred after the second hit in the wild-type *MSH6* allele, which was therefore probably an early event. The latter would fit with the MMR-DCF adenoma–carcinoma pathway, implying that most *MSH6*-associated CRCs developing through adenomas follow the MMR-DCF adenoma–carcinoma pathway rather than the adenoma–carcinoma pathway.

A limitation of this study was the number of available WES data of *MLH1*-, *MSH2*-, and *PMS2*-associated CRCs, which impeded firm comparisons with *MSH6*-associated CRCs. Although this was in part corrected by inclusion of the CHP data, the minimal coverage of the CHP data as compared with the WES data influences the quality of our mutational analysis.

In conclusion, the clinical heterogeneity observed in LS patients may be partly explained by the molecular profile of individual LS CRCs. The molecular profile of *MSH6*-associated CRCs is characterized by an abundance of dMMR signature-associated SNVs yet contains fewer dMMR signature-associated INDELs compared with *PMS2*-associated CRCs and fewer *CTNNB1* variants compared with *MLH1*-associated CRCs. Once confirmed, these findings will find application in the management of LS patients targeted to gene-specific subgroups, with the ultimate goal to fine-tune current "mismatches" in care.

Supplementary Material

Note: To access the supplementary material accompanying this article, visit the online version of *Gastroenterology* at www.gastrojournal.org and at https://doi.org/10.1053/j.gastro.2023.03.198.

NOAH C. HELDERMAN
Department of Clinical Genetics
Leiden University Medical Center
Leiden, The Netherlands

ANNE-SOPHIE VAN DER WERF-'T LAM
Department of Clinical Genetics
Leiden University Medical Center
Leiden, The Netherlands

MSH6 TUMOR GROUP

HANS MORREAU
Department of Pathology
Leiden University Medical Center
Leiden, The Netherlands

ARNOUD BOOT
Genomescan
Leiden, The Netherlands

TOM VAN WEZEL
Department of Pathology
Leiden University Medical Center
Leiden, The Netherlands

MAARTJE NIELSEN
Department of Clinical Genetics
Leiden University Medical Center
Leiden, The Netherlands

Figure 1. dMMR signature-associated variants and predicted timing of mutational events. *(A)* The total number of variants (SNVs + INDELs) was comparable between *MSH6*-associated CRCs and the other LS subgroups of the WES cohort. *(B)* The number of dMMR signature-associated SNVs was significantly higher in *MSH6*-associated CRCs (median, 387.5; interquartile range [IQR], 224–755) compared with *PMS2*-associated CRCs (median, 91; IQR, 45–101; $P < .01$) of the WES cohort. *(C)* The number of dMMR signature-associated INDELs was significantly lower in the *MSH6*-associated CRCs (median, 43; IQR, 20–63) compared with *PMS2*-associated CRCs (median, 193; IQR, 81–221; $P = .01$) of the WES cohort. The SNV mutational signatures SBS6, SBS15, SBS20, SBS21, SBS26, and SBS44 and the INDEL mutational signatures ID1, ID2, and ID7 were considered dMMR signature-associated. Statistical differences between *MSH6*-associated CRCs vs *MLH1*-, *MSH2*-, or *PMS2*-associated CRCs were evaluated using the Kruskal-Wallis test. Raw *P* values were adjusted for the number of comparisons and outcomes under investigation using Benjamini & Hochberg correction for multiple testing, are 2-tailed, and are considered significant when $P < .05$. Only significant *P* values are shown. *(D)* [1] The adenoma–carcinoma pathway is initiated by MMR-proficient adenoma formation, a process believed to be driven by *APC* variants. MMR-proficient adenomas may then acquire a second hit in the wild-type MMR allele, inducing dMMR. Consequently, genes susceptible for dMMR signature-associated variants *(i)* may accumulate variants and drive cancer outgrowth. Genes that are moderately *(ii)* or not *(iii)* susceptible to dMMR signature-associated variants may accumulate variants during any stage of tumor progression. [2] The MMR-DCF adenoma–carcinoma pathway is initiated by a second hit in the wild-type MMR allele, leading to an MMR-DCF. This MMR-DCF may acquire both dMMR signature-associated and dMMR-unrelated variants (i–iii). Once *APC* is altered, a dMMR adenoma develops, which evolves into a carcinoma on occurrence of additional cancer-driving variants. [3] Not unlike the MMR-DCF adenoma–carcinoma pathway, the MMR-DCF carcinoma pathway is initiated by a second hit in the wild-type MMR allele. However, after the accumulation of *CTNNB1* variants, the MMR-DCF may progress directly to carcinoma, surpassing an intervening adenoma stage. The 3 molecular pathway model was introduced by Ahadova et al.[8] Created with BioRender.com. *(E)* Proportion of dMMR signature-associated variants of genes with at least 5 variants in all analyzed LS CRCs. Absolute numbers are provided within bars. Variants found in WES data, which in theory would not have been covered by the CHP, were also included. According to the proportion of dMMR signature-associated variants, mutational events in genes were categorized into *(i)* dMMR signature-associated (>67% dMMR signature-associated variants), *(ii)* dMMR signature-associated/dMMR-unrelated (34%–67% dMMR signature-associated variants), and *(iii)* dMMR-unrelated (<34% dMMR signature-associated variants). (d/p)MMR, mismatch repair (deficient/proficient).

References

1. Helderman NC, et al. Crit Rev Oncol Hematol 2021;163:103338.
2. Ten Broeke SW, et al. Gastroenterology 2018;155:844–851.
3. Hendriks YM, et al. Gastroenterology 2004;127:17–25.
4. Moller P, et al. Gut 2017;66:464–472.
5. Suerink M, et al. Genet Med 2019;21:2706–2712.
6. Ten Broeke SW, et al. J Clin Oncol 2018;36:2961–2968.
7. Ahadova A, et al. Fam Cancer 2016;15:579–586.
8. Ahadova A, et al. Int J Cancer 2018;143:139–150.
9. Engel C, et al. Gastroenterology 2020;158:1326–1333.
10. Moller P, et al. Gut 2017;67:1306–1316.

Correspondence
Address correspondence to: Maartje Nielsen, MD, PhD, Department of Clinical Genetics, Leiden University Medical Center, Albinusdreef 2, 2333, Postzone K5-S, Postbus 9600, 2300 RC Leiden, The Netherlands. e-mail: m.nielsen@lumc.nl.

CRediT Authorship Contributions
Noah Cornelis Helderman, BSc, PhD candidate (Formal analysis: Lead; Investigation: Lead; Methodology: Equal; Visualization: Lead; Writing – original draft: Lead; Writing – review & editing: Lead).

Anne-Sophie van der Werf-'t Lam, MD, PhD candidate (Formal analysis: Supporting; Methodology: Supporting; Writing – original draft: Supporting; Writing – review & editing: Equal).

Diantha Terlouw, MSc, PhD candidate (Formal analysis: Supporting; Investigation: Supporting; Writing – review & editing: Equal).

Sanne W. Bajwa-ten Broeke, MD, PhD (Formal analysis: Supporting; Investigation: Supporting; Writing – review & editing: Equal).

Mar Rodríguez-Girondo, PhD (Methodology: Supporting; Writing – review & editing: Equal).

Demi van Egmond (Formal analysis: Supporting; Investigation: Supporting; Writing – review & editing: Supporting).

Alexandra M. J. Langers, MD, PhD (Writing – review & editing: Equal).

Monique E. van Leerdam, MD, PhD (Writing – review & editing: Equal).

Emily Rayner, PhD (Writing – review & editing: Equal).

Christi J. van Asperen, MD, PhD (Writing – review & editing: Equal).

Liselotte P. van hest, MD (Writing – review & editing: Supporting).

Hans J. P. Gille, PhD (Writing – review & editing: Supporting).

Floor A. M. Duijkers, MD, PhD (Writing – review & editing: Supporting).

Anja Wagner, MD, PhD (Writing – review & editing: Supporting).

Ellis L. Eikenboom, PhD candidate (Writing – review & editing: Supporting).

Tom G. W. Letteboer, PhD (Writing – review & editing: Supporting).

Mirjam M. de Jong, MD, PhD (Writing – review & editing: Supporting).

Fonnet E. Bleeker, MD, PhD (Writing – review & editing: Supporting).

Encarna B. Gomez Garcìa, MD, PhD (Writing – review & editing: Supporting).

Manon Suerink, MD, PhD (Writing – review & editing: Equal).

Carli M. Tops, PhD (Writing – review & editing: Equal).

Niels de Wind, PhD (Writing – review & editing: Equal).

Hans Morreau, MD, PhD (Conceptualization: Equal; Formal analysis: Equal; Investigation: Equal; Methodology: Equal; Writing – review & editing: Equal).

Arnoud Boot, PhD (Formal analysis: Equal; Investigation: Equal; Methodology: Equal; Writing – review & editing: Equal).

Tom van Wezel, PhD (Conceptualization: Equal; Formal analysis: Equal; Investigation: Equal; Methodology: Equal; Writing – review & editing: Equal).

Maartje Nielsen, MD, PhD (Conceptualization: Lead; Formal analysis: Equal; Funding acquisition: Lead; Investigation: Equal; Methodology: Equal; Project administration: Lead; Supervision: Lead; Writing – original draft: Supporting; Writing – review & editing: Equal).

Conflicts of interest
The authors disclose no conflicts.

Data Availability
The datasets analyzed during this study are available from the corresponding author on reasonable request.

Supplementary Methods

Ethical Statement

This study was approved by the Medical Ethical Committee of Leiden, The Hague, Delft (protocol P17.098). Patient samples were handled according to the medical ethical guidelines described in the Code of Conduct for responsible use of human tissue in the context of health research (Federation of Dutch Medical Scientific Societies). Samples were coded, and all patients provided informed consent for the use of tissue and clinical data.

Patients and Samples

The study included 106 confirmed LS CRCs, of which 44 (25 *MSH6*-, 5 *MLH1*-, 5 *MSH2*-, and 9 *PMS2*-associated CRCs) were analyzed by WES. Resultant tissue blocks were made available by various pathology departments in the Netherlands. For the remaining 62 LS CRCs, we retrieved CHP data from an earlier study by our research group.[1] This group comprised 24 *MLH1*-, 18 *MSH2*-, and 20 *PMS2*-associated CRCs. For a detailed description of the CHP analysis see Ten Broeke et al.[1]

WES Analysis

Sample preparation. For each LS CRC of the WES cohort, DNA was isolated from formalin-fixed paraffin-embedded tissue blocks of both tumor and normal tissue, using tissue cores, microdissection, or whole sections and the NucleoSpin DNA FFPE XS kit (Macherey-Nagel, Düren, DE). The Qubit Meter dsDNA High Sensitivity kit (Thermo-Fisher Scientific, Waltham, MA) was used to assess whether sufficient DNA was isolated for downstream analyses.

Molecular evaluation. WES was performed using the NovaSeq 6000 Sequencing System (Illumina Inc, San Diego, CA). Sequencing reads were trimmed using Trimomatic v.0.36[2] and aligned to GRCh38 using BWA-MEM.[3] Polymerase chain reaction duplicate removal and merging were conducted in Sambamba (v0.5.8),[4] and variant calling (ie, SNVs and INDELs) was performed using Strelka (v2.014).[5] Artifacts caused by formalin fixation were removed by reverse variant calling (ie, swapping tumor and normal) and filter optimization: Variants were filtered for variant allele frequencies of ≥10%, ≥20 times coverage in both the tumor and normal sample and at least 4 reads supporting the variant. SNVs in dbSNPv132, 1000 genomes (The 1000 Genomes Project Consortium 2015), segmental duplications, microsatellites, homopolymers, and the GL and KI sequences were excluded.

Variant annotation and the removal of (likely) benign variants were performed using ANNOVAR.[6] First, we developed a pipeline within ANNOVAR and data parser (source code available on request) that selected non-synonymous or splice variants, which were not located in segmental duplications and not observed in the Exome Aggregation Consortium[7] and/or Exome Sequencing Project[8] with an allele frequency higher than 1%. Databases used for this pipeline were downloaded from ANNOVAR

directly or were retrieved from the University of California, San Diego Genome Browser Annotation Database.[9] Next, variants were selected if located in any of 205 well-known onco- and tumor suppressor genes. This list of genes was created primarily by extracting the overlapping genes from the TruSight Oncology 500 Assay (Illumina), the Oncomine Tumor Mutation Load Assay (ThermoFisher Scientific), MSK-IMPACT,[10] and the Cancer Gene Census[11] (list available upon request). The selected variants were visualized and validated using Integrative Genomics Viewer.[12] Variants with a variant allele frequency < 20%, <3 unique reads on both the plus and minus strands, and/or a read difference > 1:7 between both strands were not considered. Finally, variants were classified according to the American College of Medical Genetics and Genomics recommendations for variant interpretation using Franklin.[13,14] Variants reported in this study classify as variants of unknown significance, likely pathogenic or pathogenic, and in addition have a combined annotation-dependent depletion score higher than 20, indicating they are considered to be in the top 1% of possibly pathogenic variants.[15]

LOH of the MMR genes was manually curated with the use of Integrative Genomics Viewer.[12] LOH was considered when the variant allele frequency of the germline MMR variant differed ≥20% between tumor and normal tissue or when at least 4 of 10 randomly assessed single-nucleotide polymorphisms, located both upstream and downstream of the MMR variant, showed a variant allele frequency difference of ≥20% between tumor and normal tissue.

Mutational Signature Analysis

Overall. Mutational signatures were extracted from the WES data to score the overall contribution of dMMR to the total number of variants in each LS CRC of the WES cohort, using SigProfiler and the SigProfiler reference mutational signatures.[16] The SNV mutational signatures SBS6, SBS15, SBS20, SBS21, SBS26, and SBS44 and the INDEL mutational signatures ID1, ID2, and ID7 were considered dMMR signature-associated. SBS1, SBS5, and SBS40 were considered to be aging-related.[16–20]

Gene based. For each gene with at least 5 variants in the combined WES and CHP cohorts, we estimated the proportion of dMMR signature-associated variants to analyze the sequence of mutational events. SNVs were considered dMMR signature-associated when they involved C>T (G>A) transitions at NpCpG or GpCpN trinucleotide contexts, corresponding with SBS6.[16–20] INDELs were considered dMMR signature-associated if they involved single-nucleotide INDELs affecting homopolymer sequences (≥4 bp), corresponding with ID1, ID2, and ID7.[16–20]

Statistical Analysis

Statistical analyses were performed using IBM SPSS Statistics for Windows 2017 (version 25.0) and RStudio (Team R, Integrated Development for R, Boston, MA, 2020). Continuous outcomes are presented as median

(interquartile range) and were compared using the Mann-Whitney U test (2 groups) or Kruskal-Wallis test ($>$2 groups). Categorical outcomes are presented as proportions and were compared using Fisher's exact test (2 categories) or Pearson's χ^2 test ($>$2 categories). Outcomes were compared between *MSH6*-associated CRCs vs *MLH1*-, *MSH2*-, or *PMS2*-associated CRCs, and raw *P* values were subsequently adjusted for the number of comparisons and outcomes under investigation using Benjamini & Hochberg correction for multiple testing. In the combined WES and CHP data analysis, variants observed in the WES cohort were only taken into account if the chromosome position was covered in the CHP. The latter does not apply for the gene-based signature analysis. All *P* values mentioned in this article are 2-tailed and considered statistically significant when $P < .05$.

Supplementary References

1. Ten Broeke SW, et al. Gastroenterology 2018; 155:844–851.
2. Bolger AM, et al. Bioinformatics 2014;30:2114–2120.
3. Li H, et al. Bioinformatics 2009;25:1754–1760.
4. Tarasov A, et al. Bioinformatics 2015;31:2032–2034.
5. Saunders CT, et al. Bioinformatics 2012;28:1811–1817.
6. Wang K, et al. Nucleic Acids Res 2010;38:e164.
7. Genomes Project Consortium, et-al. Nature 2010; 467:1061–1073.
8. NHLBI GO ESP Project. https://esp.gs.washington.edu/drupal/node/1.
9. Karolchik D, et al. Nucleic Acids Res 2014; 42:D764–D770.
10. Cheng DT, et al. J Mol Diagn 2015;17:251–264.
11. Sondka Z, et al. Nat Rev Cancer 2018;18:696–705.
12. Robinson JT, et al. Nat Biotechnol 2011;29:24–26.
13. Franklin by genoox. https://franklin.genoox.com/clinical-db/home.
14. Richards CS, et al. Genet Med 2008;10:294–300.
15. Rentzsch P, et al. Nucleic Acids Res 2019; 47:D886–D894.
16. Alexandrov LB, et al. Nature 2020;578:94–101.
17. Alexandrov LB, et al. Nature 2013;500:415–421.
18. ICGC/TCGA Pan-Cancer Analysis of Whole Genomes Consortium. Nature 2020;578:82–93.
19. Tate JG, et al. Nucleic Acids Res 2019;47:D941–D947.
20. Diaz-Gay M, et al. Adv Cancer Res 2021;151:385–424.